A peer-reviewed version of this preprint was published in PeerJ on 1 November 2016.

View the peer-reviewed version (peerj.com/articles/2458), which is the preferred citable publication unless you specifically need to cite this preprint.

Zancopé BR, Dainezi VB, Nobre-dos-Santos M, Duarte S Jr., Pardi V, Murata RM. 2016. Effects of CO_2 laser irradiation on matrix-rich biofilm development formation–an in vitro study. PeerJ 4:e2458 https://doi.org/10.7717/peerj.2458

Effects of CO_2 laser irradiation on matrix-rich biofilm development formation – An *in vitro* study

Bruna Raquel Zancope, Vanessa B Dainezi, Marinês Nobre-dos-Santos, Sillas Duarte-Junior, Vanessa Pardi, Ramiro M Murata

Background. CO2 laser has been used to morphologically and chemically modify the dental enamel surface as well as to turn it more resistant to demineralization. Despite a variety of experiments demonstrating the inhibitory effect of CO2 laser in reduce enamel demineralization, little is known about the effect of surface irradiated on bacterial growth. Thus, this in vitro study was preformed to evaluate the biofilm formation on enamel previously irradiated with a CO2 laser (λ = 10.6 μM). Methods. For this in vitro study, it was employed 96 specimens of bovine enamel, which were divided into 2 groups (n = 48): 1) Control-non-irradiated surface and 2) Irradiated enamel surface. Biofilms were grown on the enamel specimens by 1, 3 and 5 days under intermittent cariogenic condition in the irradiated and non irradiated surface. In each assessment time, the biofilm were evaluated by dry weigh, counting the number of viable colonies and in fifth day, were evaluated by polysaccharides analysis, quantitative real time PCR as well as by contact angle. In addition, the morphology of biofilms was characterized by fluorescence microscopy and field emission scanning electron microscopy (FESEM). Initially, the assumptions of equal variances and normal distribution of errors were conferred and the results are analyzed statistically by t-test and Mann Whitney test. Results. The mean of log CFU/ml obtained for the 1-day biofilm evaluation showed that there is statistical difference between the experimental groups. When biofilms were exposed to CO2 laser, CFU/mL and CFU/ Dry Weight in 3 day was reduced significantly compared with control group. The difference in the genes expression (gtfB and gbpB) and polysaccharides was not statically significant. Contact angle was increased relative to control when the surface was irradiated with CO2 laser. Similar morphology was also visible with both treatments, however irradiated group revealed evidence of melting and fusion in the specimens. Conclusion. In conclusion CO2 laser irradiation modify the energy surface and disrupt the initial biofilm formation.

PeerJ Preprints | https://doi.org/10.7287/peerj.preprints.2084v1 | CC-BY 4.0 Open Access | rec: 30 May 2016, publ: 30 May 2016

Effects of CO_2 Laser Irradiation on Matrix-Rich Biofilm Development Formation – An *in vitro* study.

Bruna Raquel Zancopé[a], Vanessa Benetello[a], Marinês Nobre-dos-Santos[a], Sillas Duarte[b], Vanessa Pardi[c], Ramiro Mendonça Murata[c].

[a]Department of Pediatric Dentistry, Piracicaba Dental School, University of Campinas-UNICAMP, Av. Limeira 901, Piracicaba-SP, Brazil, CEP 13414-903;
[b]Division of Restorative Sciences, Ostrow School of Dentistry of University of Southern California, 925 W. 34th Street, Los Angeles-LA, United States, 90089.
[c]Division of Periodontology, Diagnostic Sciences and Dental Hygiene, Ostrow School of Dentistry of University of Southern California, 925 W. 34th Street, Los Angeles-LA, United States, 90089.

Corresponding Author
Ramiro Mendonça Murata
University of Southern California- Herman Ostrow School of Dentistry
Division of Periodontology Diagnostic Sciences, Dental Hygiene and Biomedical Science
925 W. 34th Street, DEN 4108
Los Angeles, CA 90089
E-mail: ramiro.murata@usc.edu
Tel: +1 (213) 740-3867
Fax: +1 (213) 740-8416

Abstract

Background. CO_2 laser has been used to morphologically and chemically modify the dental enamel surface as well as to render it more resistant to demineralization. Despite a variety of experiments demonstrating the inhibitory effect of CO_2 laser in the reduction of enamel demineralization, little is known on the effect of surface irradiated on bacterial growth. Thus, this *in vitro* study was preformed to evaluate the biofilm formation on enamel previously irradiated with a CO_2 laser ($\lambda = 10.6$ μM).

Methods. In this *in vitro* study, 96 specimens of bovine enamel were divided into 2 groups (n = 48): control non-irradiated surface and irradiated enamel surface. Biofilms were grown on the enamel specimens by 1, 3 and 5 days under intermittent cariogenic condition in the irradiated and non-irradiated surface. On each respective day, dry weight and the number of viable colonies of the biofilm were assesessed while on the fifth day, polysaccharides analysis, quantitative real time PCR and contact angle were evaluated. In addition, the morphology of biofilms was characterized by fluorescence microscopy and field emission scanning electron microscopy (FESEM). Initially, the assumptions of equal variances and normal distribution of errors were conferred and the results are analyzed statistically by t-test and Mann Whitney test.

Results. The mean of log CFU/ml obtained for the 1-day biofilm evaluation showed that there is statistical difference between the experimental groups. When biofilms were exposed to CO_2 laser, CFU/mL and CFU/ Dry Weight in 3 day was reduced significantly compared to the control group. The difference in the genes expression (gtfB and gbpB) and polysaccharides were not statically significant. Contact angle was increased relative to control when the surface was irradiated with CO_2 laser. Similar morphology was also visible with both treatments; however, the irradiated group revealed evidence of melting and fusion in the specimens.

Conclusion. In conclusion, CO_2 laser irradiation can modify the energy surface and disrupt the initial biofilm formation.

Introduction

Dental caries, a biofilm-related disease, remains among the most prevalent human infections disease affecting both children and adults worldwide (Do 2012; Dye et al. 2008; Marcenes et al. 2013). Despite its decline over the last decades primarily due to the widespread use of fluoride compounds, caries disease activity in children is as high as 60 to 70% (Murata & Pardi 2007; Taubman & Nash 2006) (García-Godoy & Hicks 2008; Greene 2005; Hausen 1997; WHO 2003). Colonization of tooth surfaces by *mutans streptococci* and its interaction with constituents from the host's diet is associated with the etiology and pathogenesis of dental caries in humans (Bowen ; Marsh). Although dental biofilms are composed of diverse and complex oral microorganisms, *Streptococcus mutans* is considered the primary etiologic agent of dental caries, which has an important role in the initiation and progression of the dental caries (Loesche 1986; Wang et al. 2013), as it uses carbohydrates, such sucrose, to synthesize extracellular polysaccharides and can survive under low pH conditions, leading to enamel demineralization (Rolla 1989).

Laser therapy has been studied as a promising alternative in the prevention of caries. Different types of lasers such as Nd: YAG, Argon, Er: YAG and CO_2 have been studied for their potential use in dentistry. The use of high power lasers has been suggested as the treatment of tooth enamel in order to obtain more resistant surfaces to acids produced by cariogenic bacteria (Featherstone et al. 1991; Featherstone et al. 1998; Hsu et al. 2000; Kantorowitz et al. 1998). A study conducted by Armengol et al., (2003) showed that morphological changes on enamel and dentin were greater when Er:YAG laser and Nd:YAP laser were employed, which was asscociated with a greater free surface energy. Intriguingly, Venault et al., (2014) reported that the coating of hydroxyapatite with a polyethyleneimine (PEI) polymer inhibited the adsorption and showed a 70% inhibition of oral bacterial adhesion on human teeth. However, the applicability of superhydrophobic and superhydrophilic surfaces in the dental field remains to be investigated. The conventional wisdom is that a reduction of surface roughness and surface free energy of a dental material coincides with a decrease in microbial adherence and proliferation (Buergers et al. 2009; Teughels et al. 2006). These results suggest that surface parameters such

as the chemical composition and topography might be key parameters for optimizing the enamel surface properties in order to reduce biofilm formation on their surfaces.

The carbon dioxide laser (CO_2) acts on enamel demineralization to reduce the acid solubility. Previous studies have also shown significant inhibition of enamel demineralization following treatment with a CO_2 laser (Hsu et al. 2001; Nobre-dos-Santos et al. 2001; Rodrigues et al. 2006; Steiner-Oliveira et al. 2006; Tagliaferro et al. 2007). There are several hypotheses that attempt to explain the mechanisms by which CO_2 laser inhibits tooth enamel demineralization. One possible explanation is based on reducing enamel solubility caused by the melting and recrystallization of hydroxyapatite crystals (Nelson et al. 1986). However, there is no report in the scientific literature showing whether these morphological alterations promoted by laser irradiation could change the energy surface and consequently to modify the development of biofilm enamel surface. Thereby, the aim of this study was to evaluate the biofilm formation on enamel previously irradiated with a CO_2 laser ($\lambda = 10.6$ μm).

Material and Methods

Experimental design

Ninety-six dental enamel specimens were previously prepared were randomly allocated in two groups (n=48): 1) Control-non-irradiated surface and 2) Irradiated enamel surface. Biofilms were grown on the enamel specimens by 1, 3 and 5 days under intermittent cariogenic condition in the irradiated and non-irradiated surface. The following analyses were performed: adherence test with 1-day biofilm formation (n=8), bacterial viability, colony forming units - CFU/mg of biofilm dry weight, dry weight and polysaccharides analysis with 3-day (n=10) and 5-day (n=10) biofilm formation. Real time PCR (n=9) and Contact angle (n=6). Morphological surface changes of 3 specimens of each group were examined by Field Emission Scanning Electron Microscopy and by fluorescence microscopy (Figure 1).

Tooth selection and sample preparation, experimental model

To perform this *in vitro* study, 96 sound bovine incisors that were free from caries, macroscopic cracks, abrasions as well as staining assessed by visual examination, were stored in a 0.1% thymol solution, and sectioned mesiodistally using a water-cooled diamond saw in a

cutting machine (Isomet, Buehler, Lake Bluff, Ill, USA). The tooth halves were polished for 30s using a 5µm alumina/water suspension micropolish (Instrumental, Jabaquara, SP, Brazil) to expose fresh enamel. The specimens were coated with an acid-resistant varnish leaving a window of 4 mm^2 of exposed enamel in the middle of the surface. The teeth were sterilized using oxide ethylene (Acecil. Com. Ind. Ltda. Campinas-SP, Brasil).

Laser irradiation parameters

For this study, we based the irradiation parameters in a previous work by our group (Steiner-Oliveira et al. 2006) showing that 11.3 J/cm^2 was able to produce chemical and morphological changes that could reduce the acid reactivity of enamel without compromising pulp vitality. The enamel surface irradiation was performed using an X-Y positioning platform at a 10-mm distance from the tip of the handpiece. The scanning speed was approximately 1 mm/s and total irradiation time was 30 s. To perform enamel surface irradiation, a pulsed CO_2 laser at 10.6µm wavelength (Union Medical Engineering Co. Model UM-L30, Yangju-si, Gyeonggi-Do, Korea) was used with the following parameters: 10-ms pulse duration, 10-ms of time off, 50-Hz repetition rate, beam diameter of 0.3-mm. Using a power meter (Scientech 373 Model-37-3002, Scientech Inc., Boulder, CO, USA). The average power output was measured at 0.4 W for the correspondent lased groups was measured using a power meter (Scientech 373 Model-37-3002, Scientech Inc., Boulder, CO, USA). The fluency laser point applied on enamel was 11.3 J/cm^2. We performed an overlap between the irradiation points, but without the central area. The central point of irradiation is the area getting the most uniform power. Around the center, there is a loss of energy, which is where the overlap of the next beam was performed (Figure 2).

Biofilm formation and analysis

Streptococcus mutans UA159 (ATCC 700610), a virulent cariogenic pathogen, was used for the biofilm study. Biofilms were grown in Brain Heart Infusion (BHI) broth containing 1% (w/v) sucrose and were kept undisturbed for 24 h to allow initial biofilm formation. Medium was replaced twice daily. Biofilms of *S. mutans* UA159 were formed on specimens of bovine enamel placed in 2 mL of medium containing 1% sucrose, in 24-well cell culture plates, at 37°C, 5% CO_2, for 3 and 5 days, which were dip-washed three times with PBS (Phosphate Buffered Saline)

at the end of each experimental period. The biofilms were removed using a metallic spatula, immersed in a falcon tube with PBS and subjected to sonication using three 15 s pulses at an output of 7 W (Fisher Scientific, Sonic Dismembrator model 100; USA). The suspension was used as previously described (Duarte et al. 2006) for dry weight, bacterial viability (colony forming units—CFU/mg of biofilm dry weight), and polysaccharide analyses (EPS-soluble, EPS-insoluble and intracellular polysaccharides—IPS) (Duarte et al. 2011).

S. mutans adherence test was performed in day 1 of biofilm formation. After that, the numbers of colonies were counted and the value of log CFU/mL was calculated (Branco-de-Almeida et al. 2011).

Dry weight and Bacterial viability

Three volumes containing cold ethanol (-20°C) were added to 1 mL biofilm suspension, and the resulting precipitate was centrifuged (10,000 g for 10 min at 4°C). The supernatant was discarded, and the pellet was washed with cold ethanol, and then lyophilized and weighed (Duarte et al. 2006).

An aliquot (0.1 mL) of the homogenized suspension was serially diluted (1:10, 1:100, 1:1000, 1:10000, 1:100000, 1:1000000) and plated on blood agar. The plates were incubated in 5% CO_2 at 37°C for 48 h, and the number of CFU mg-1 of biofilm dry weight were determined (Murata et al. 2010).

Polysaccharide analysis

Soluble and insoluble extracellular polysaccharides (EPS-soluble and EPS-insoluble) were analyzed as previously described (Duarte et al. 2006). The polysaccharide content was expressed per mg of polysaccharide by dry weight of total biofilm. Briefly, an aliquot (2 mL) of the suspension was sonicated for 30 s pulses at an output of 7 W and centrifuged at 10,000 g for 10 min at 4°C. The supernatant was collected and the biofilm pellet was resuspended and washed in 5 mL of milli-Q water. This procedure was repeated three times. The supernatant was used for the EPS-soluble assay and biofilm pellet was used for the EPS-insoluble assay. All of the supernatants were pooled and three volumes of cold ethanol were added, and the resulting precipitate was collected by centrifugation and resuspended in 5 mL Milli-Q water; the total amount of carbohydrate was determined by the phenol—sulfuric acid method (Dubois et al.

1951). The EPS-insoluble was extracted using 1 N NaOH (1 mg biofilm dry weight/0.3 mL of 1 N NaOH) under agitation for 1 h at 37°C. The supernatant was collected by centrifugation, and the precipitate was resuspended again in 1N NaOH; this procedure was repeated three times. The total amount of carbohydrate was determined by colorimetric method with phenol sulfuric acid (Dubois et al. 1951).

Quantitative Real-Time PCR

All RNA was isolated from biofilm (3 days). The *S. Mutans* RNA were isolated and purified by using the Ribopure Kit (Life Technology, Grand Island, NY, USA). A NanoPhotometer P360 (Implen, Westlake Village, CA, USA) was used to quantify the total RNA extracted. Reverse transcription of the RNA into cDNA was carried out by using iScript Advanced cDNA synthesis Kit for RT-qPCR (Biorad, Hercules, CA, USA) according to the manufacture's instructions. Real-time PCR was conducted by using iQ SYBR Green Supermix (Biorad, Hercules, CA, USA) (Klein et al. 2010). The *S. Mutans* primers for the genes: Glucosyltransferase (gtfB), Glucan-binding protein (gbp), at 10 μM were used. The standard curves were used to transform the critical threshold cycle (Ct) values to the relative number of cDNA molecules. Relative expression was calculated by normalizing each gene of interest to the *S. mutans* 16S rRNA gene, which is a well-established reference gene (Table 1). PCR amplification was performed by using 20 μL reaction mix per well in a 96 well plate. The reactions were conducted at 95 °C for 3 minutes, followed by 40 cycles of 15 seconds at 95 °C and 1 minute at 60 °C. After PCR, the melting curve was obtained by incubating the samples at increasing increments of 0.5 °C from 55 °C to 95 °C (Klein et al. 2009; Koo et al. 2006).

Contact Angle – Wettability Measurement

Wettability of enamel after treatments was evaluated by contact angle measurements. The sessile drop method was performed using Digidrop GBX goniometer (Labometric Lda, Leiria, Portugal) with enamel surface (control and laser). Briefly, deionized water was loaded into a 3 mL syringe (Luer-Lok™ Tip, BD, Franklin Lakes, NJ, USA) and coupled to the goniometer. Droplets (≅ 1 μL) were careful applied on the different enamel surfaces using a 22-gauge needle (Injex Ltda, São Paulo, SP, Brazil). Ten drops of water were dispensed on the enamel surface. The measurement of contact angle was accomplished immediately after the water drop has

formed on enamel surface. The test was accomplished at room temperature and the drop images captured without external lights interferences. Images were frozen by PixeLink system (Barrington, IL, USA) and the measurements were made by the GBX Digidrop Windrop software (GBX Company, Bourg de Péage, France). The focus of camera used to capture the images was adjusted in relation to the position of the table with glass slide surface and the needle tip. The right and left angles were measured in degrees of the contact angle and average automatically calculated by GBX Digidrop software (GBX Company, Bourg de Péage, France). The average obtained from each specimen and from each group was submitted to statistical analysis (Paris et al. 2007).

Field Emission Scanning Electron Microscopy

This analysis aimed to evaluate the surface of specimens after CO_2 LASER irradiation and biofilm formation. All specimens were first mounted on aluminum stubs and sputter-coated with gold (~10-12 nm thickness) using a BAL-TEC SCD 050 sputter coater (Wetzlar, Liechtenstein/Vienna, Austria). Observations were made with a JEOL JSM-7001 Field Emission Scanning Electron Microscope (Jeol, Peabody, MA, USA) operating at 15 kV and using magnifications up to 2500X (Weber et al. 2014).

Fluorescence Microscopy

The distribution of dead and live *S. mutans* was examined after 1, 3 and 5 days of biofilm using the Viability/Cytotoxicity Assay Kit LIVE/DEAD® BacLight™ Bacterial Viability (Life Technologies, Carlsbad, CA, USA) for microscopy which contains a The LIVE/DEAD BacLight Bacterial Viability Kits employ two nucleic acid stains — the green-fluorescent SYTO® 9 stain and the red-fluorescent propidium iodide stain. These stains differ in their ability to penetrate healthy bacterial cells. When used alone, SYTO 9 stain labels both live and dead bacteria. In contrast, propidium iodide penetrates only bacteria with damaged membranes, reducing SYTO 9 fluorescence when both dyes are present. Thus, live bacteria with intact green membranes fluoresce, while dead bacteria with damaged membranes fluoresce red were evidenced. Fluorescent images of the double staining were captured using fluorescence microscopy (EVOS fl microscope AMG, Bothell, WA, USA). (Rolland et al. 2006).

Statistical analysis

The Lilliefors test showed that data of CFU, CFU/ dry weight on day 3, dry weight on day 5 and insoluble polysaccharide did not follow normal distribution and were analyzed by Mann-Whitney test. Results of adherence test on day 1, dry weight on day 3, CFU, CFU/ dry weight on day 5, soluble polysaccharides, real time PCR and contact angle did follow normal distribution and were analyzed by T-test, Data normality and the other analyses were performed using BioEstat 5.0 (Mamirauá, Belém, PA, Brazil) with a 5% significance level.

To evaluate the surface of specimens after treatments and biofilm formation and distribution of dead and live *S. mutans* after 1, 3 and 5 days of biofilm formation, field emission scanning electron and fluorescence microscopy were respectively performed for illustration.

Results

Table 2 showed, the results of 3 and 5 days of biofilm formation. The results on day 3 showed that the values of CFU/ mL for irradiated group were significantly ($p < 0.05$) less when compared to the control group. The normalized data (CFU/Dry Weight) showed noteworthy reduction ($p < 0.05$) by the irradiation on day 3. However, no statistical difference was found between the groups in day 3 for Dry Weight values ($p > 0.05$). There were no statistical difference found between the groups in CFU/ mL, Dry Weight and CFU/ Dry Weight on day 5 ($p > 0.05$).

The results obtained for the analysis of *S. mutans* adherence to enamel surface after laser irradiation and biofilm formation are presented in Figure 3. The values of log CFU/mL obtained for the 1-day biofilm evaluation showed that although the difference between the means had been small (control group Log= 6.06±0.23, irradiated group Log= 5,56±0,35) there is statistical difference between the 2 groups ($p < 0.05$).

Table 3 showed that soluble and insoluble polysaccharides (µg PSA/ mg dry weight) were unaffected by enamel irradiation ($p > 0.05$).

Contact Angle – Wettability Measurement analysis results after enamel treatment were shown in Table 4. This result showed that contact angle was higher for the irradiated group (87.6 ± 9.41) than for the control group (76.0 ± 3.33) and the difference between the 2 groups was statistically significant ($p < 0.05$).

To assess the effect of CO_2 laser irradiated surface on *S. mutans* gene expression we used quantitative real time PCR. We compared control non-irradiated samples to irradiated samples. The difference in the genes expression (gtfB and gbpB) was not statically significant (Fig. 4).

Fluorescence Microscopy representative images of bacteria in biofilms after 1, 3 and 5 days of biofilm were shown in Figure 5. Multidimensional imaging of live (Green) and dead (red) bacteria can be observed at different times of *S. mutans* biofilm. Similar results were found in both groups of treatment. Biofilms formed on specimens became denser from day 1 to day 5. The image on day 1 showed primarily few amounts of live bacteria, with no dead cells. In contrast, substantial increases in dead bacteria occurred with the increase of the days. In the last day (day 5), biofilms consisted of primarily dead bacteria, connected with each other to form twisted strings. Other aspect that is possible to observe is that on day 3 the dead cell (red) were located inside the biofilm while the live cells were externalized, however on day 5 occurred the predominance of dead cells.

The SEM images of each group at different time points were shown in Figure 6. The images illustrated the effects of enamel CO_2 laser irradiation on the morphology and structure on *S. mutans* biofilm. On day 1, both groups had less bacteria in the biofilm than the day 3 and 5. Specimens with 5 days biofilm presented a thick and dense biofilm. Irradiated group had biofilms similar to those of composite control in both days. However, on day 1, the SEM observation revealed evidence of melting and fusion in the specimens treated with the CO_2 laser.

Discussion

Laser irradiation has long been used in medicine and lately also in the dental field. Some of these applications are intended for areas where bacteria are harbored or used directly to eradicate bacteria from infected areas (Sol et al. 2011). Another aspect to consider is that the critical pH (5.5) for the dissolution of enamel is reduced to 4.8 after irradiation with CO_2 laser (Fox et al. 1992). Despite a variety of experiments demonstrating the inhibitory effect of CO_2 laser in reducing enamel demineralization, little is known about the effect of surface irradiation on bacterial growth.

The wavelengths obtained with CO_2 lasers (λ = 9.3, 9.6, 10.3 and 10.6 μM) produce radiation in the infrared region, which coincides with some absorption bands of hydroxyapatite, particularly the carbonate and phosphate groups (Rodrigues et al. 2006). When the light is

absorbed in a few external micrometers from the surface of the tooth and converted the enamel, a heat loss occurs in mineral carbonate as well as fusion of the hydroxyapatite crystals, resulting in a decrease of acid reactivity in this structure (Fried et al. 1997). The reduced solubility of spent enamel has also been attributed to melting and recrystallization of the crystals (Nelson et al. ; Nelson et al.). These morphological changes can interfere in the default adhesion of bacterial cells to the tooth surface, which is essential to early carious lesions formation (Newbrun 1977).

Adhesion is the initial step in biofilm formation. Thus, an understanding of bacteria-surface interactions is essential for biofilm control. Bacterial cells approach surfaces by different means, including sedimentation, movement with liquid flow, bacterial motility with cell surface appendages, and interaction with other cells to form aggregates (Teughels et al. 2006). In this study, initial adhesion in day 1 of biofilm formation was investigated and the data revealed that laser irradiation decreased the initial cell adherence of *Streptococcus mutans*. On day 3, it is possible to observe a greater value of biofilm formation in control group. However, with the progression of time, at day 5, this difference becomes less visible and is statistically similar.

The formation and composition of biofilm appear to vary on different surfaces (Aroonsang et al. 2014) and effects of material/surface properties, such as surface charge, hydrophobicity, roughness, topography, and chemistry on bacterial adhesion and biofilm formation have been investigated for many years (Anselme et al. ; Badihi Hauslich et al. ; Guegan et al. ; Perera-Costa et al. ; Song & Ren). These factors may be interrelated, which may explain the inhibition of biofilm formation found on irradiated enamel.

The role of hydrophobicity in oral bacterial adhesion has been reviewed elsewhere (Busscher et al. ; Busscher et al. ; Nobbs et al.). In general, by tuning the hydrophobicity of a surface, bacterial adhesion can be inhibited. The results of this present study indicated that laser irradiation was able to increase the hydrophobicity of the enamel when compared to the control group. This finding was in agreement with a previous report by Quirquen et al., (1996), who showed that in oral environments on supragingival surfaces, less biofilm is formed on hydrophobic surfaces than hydrophilic ones. This increase of the hydrophobicity on irradiated enamel can be related to the decrease in initial biofilm formation which was found in this study.

Gene expression in bacteria can be affected by light and laser irradiation (Steinberg et al.). However, how bacteria sense and respond to different surface properties at the genetic level is largely unknown. *S. mutans* does not always dominate within dental plaque, but it is

recognized that glucosyltransferases (Gtfs) from *S. mutans* play critical roles in the development of virulent dental plaque. These Gtf genes, among other functions, are responsible for producing the soluble and insoluble polysaccharides matrix. The EPS-insoluble plays a significant role on *S. mutans* adhesion and accumulation on the tooth surface (Bowen & Koo 2011). In addition, it potentially changes the biofilm structure, resulting in increased porosity (Dibdin & Shellis 1988), which allows fermentable substrates to diffuse and be metabolized in the deepest parts of the biofilm (Zero et al. 1986). The present study demonstrated that irradiating enamel surface with laser irradiation did not affect the gene expression of GtfB and consequently, did not change the production of polysaccharides. Conversely, synthesis of glucan binding proteins (Gbps) may enhance the ability of *S. mutans* to interact with the EPS-rich matrix (Banas & Vickerman 2003). The adhesion between the bacterial cells and the EPS-matrix may be partially mediated by cell-surface GbpC, and possibly GbpB whereas secreted GbpA and GbpD may be cross-linked with the matrix contributing to the maintenance of the biofilm architecture (Lynch et al. 2007). The amounts of GbpB observed in irradiated enamel do not have direct implications for the biofilm morphogenesis and structural integrity (Duque et al. 2011).

To determine the morphology of *S. mutans* biofilms with respect to topography, we used SEM microscopy. In our study, the *S. mutans* biofilm topography was visibly not altered after laser irradiation, in both fluorescence microscopy and SEM images. This result suggests that although the laser irradiation promoted surfaces alteration such as fusion and melt, which is visible in MEV it did not promote disorganization and disaggregation of the microorganisms in the biofilm, inhibiting their growth and metabolism.

To the best of our knowledge, this is the first report of CO_2 laser irradiation effect on the prevention of oral biofilm development. Laser irradiation modified *S. mutans* biofilm development by reducing its formation. Our findings suggest that bacteria have complex systems to sense and respond to environmental challenges. The interplay between how surface properties and pellicle formation affect the bacterial adhesion strength, the mechanical stability, and detachment of biofilms, is an area that needs to be elucidated. In conclusion, CO_2 laser irradiation can modify the energy surface and disrupt the initial biofilm formation.

References

373 Anselme K, Davidson P, Popa AM, Giazzon M, Liley M, and Ploux L. 2010. The interaction of
374 cells and bacteria with surfaces structured at the nanometre scale. *Acta Biomater* 6:3824-
375 3846. 10.1016/j.actbio.2010.04.001
376 Armengol V, Laboux O, Weiss P, Jean A, and Hamel H. 2003. Effects of Er:YAG and Nd:YAP
377 laser irradiation on the surface roughness and free surface energy of enamel and dentin:
378 an in vitro study. *Oper Dent* 28:67-74.
379 Aroonsang W, Sotres J, El-Schich Z, Arnebrant T, and Lindh L. 2014. Influence of substratum
380 hydrophobicity on salivary pellicles: organization or composition? *Biofouling* 30:1123-
381 1132. 10.1080/08927014.2014.974155
382 Badihi Hauslich L, Sela MN, Steinberg D, Rosen G, and Kohavi D. 2013. The adhesion of oral
383 bacteria to modified titanium surfaces: role of plasma proteins and electrostatic forces.
384 *Clin Oral Implants Res* 24 Suppl A100:49-56. 10.1111/j.1600-0501.2011.02364.x
385 Banas JA, and Vickerman MM. 2003. Glucan-binding proteins of the oral streptococci. *Crit Rev*
386 *Oral Biol Med* 14:89-99.
387 Bowen WH. 2002. Do we need to be concerned about dental caries in the coming millennium?
388 *Crit Rev Oral Biol Med* 13:126-131.
389 Bowen WH, and Koo H. 2011. Biology of Streptococcus mutans-derived glucosyltransferases:
390 role in extracellular matrix formation of cariogenic biofilms. *Caries Res* 45:69-86.
391 10.1159/000324598
392 Branco-de-Almeida LS, Murata RM, Franco EM, dos Santos MH, de Alencar SM, Koo H, and
393 Rosalen PL. 2011. Effects of 7-epiclusianone on Streptococcus mutans and caries
394 development in rats. *Planta Med* 77:40-45. 10.1055/s-0030-1250121
395 Buergers R, Schneider-Brachert W, Hahnel S, Rosentritt M, and Handel G. 2009. Streptococcal
396 adhesion to novel low-shrink silorane-based restorative. *Dent Mater* 25:269-275.
397 10.1016/j.dental.2008.07.011
398 Busscher HJ, Norde W, and van der Mei HC. 2008. Specific molecular recognition and
399 nonspecific contributions to bacterial interaction forces. *Appl Environ Microbiol*
400 74:2559-2564. 10.1128/AEM.02839-07
401 Busscher HJ, Rinastiti M, Siswomihardjo W, and van der Mei HC. 2010. Biofilm formation on
402 dental restorative and implant materials. *J Dent Res* 89:657-665.
403 10.1177/0022034510368644
404 Dibdin GH, and Shellis RP. 1988. Physical and biochemical studies of Streptococcus mutans
405 sediments suggest new factors linking the cariogenicity of plaque with its extracellular
406 polysaccharide content. *J Dent Res* 67:890-895.
407 Do LG. 2012. Distribution of caries in children: variations between and within populations. *J*
408 *Dent Res* 91:536-543. 10.1177/0022034511434355
409 Duarte S, Gregoire S, Singh AP, Vorsa N, Schaich K, Bowen WH, and Koo H. 2006. Inhibitory
410 effects of cranberry polyphenols on formation and acidogenicity of Streptococcus mutans
411 biofilms. *FEMS Microbiol Lett* 257:50-56. 10.1111/j.1574-6968.2006.00147.x
412 Duarte S, Kuo S, Murata R, Chen C, Saxena D, Huang K, and Popovic S. 2011. Air plasma
413 effect on dental disinfection. *Physics of Plasmas* 18.
414 Dubois M, Gilles K, Hamilton J, Rebers P, and Smith F. 1951. A colorimetric method for the
415 determination of sugars. Nature.
416 Duque C, Stipp RN, Wang B, Smith DJ, Höfling JF, Kuramitsu HK, Duncan MJ, and Mattos-
417 Graner RO. 2011. Downregulation of GbpB, a component of the VicRK regulon, affects

biofilm formation and cell surface characteristics of Streptococcus mutans. *Infect Immun* 79:786-796. 10.1128/IAI.00725-10

Dye BA, Nowjack-Raymer R, Barker LK, Nunn JH, Steele JG, Tan S, Lewis BG, and Beltran-Aguilar ED. 2008. Overview and quality assurance for the oral health component of the National Health and Nutrition Examination Survey (NHANES), 2003-04. *J Public Health Dent* 68:218-226. 10.1111/j.1752-7325.2007.00076.x

Featherstone J, Zhang S, Shariati M, and McCormack S. 1991. Carbon dioxide laser effects on caries-like lesions of dental enamel. Lasers Orthop Dent Vet Med SPIE. p 145-149.

Featherstone JD, Barrett-Vespone NA, Fried D, Kantorowitz Z, and Seka W. 1998. CO2 laser inhibitor of artificial caries-like lesion progression in dental enamel. *J Dent Res* 77:1397-1403.

Fox JL, Yu D, Otsuka M, Higuchi WI, Wong J, and Powell G. 1992. Combined effects of laser irradiation and chemical inhibitors on the dissolution of dental enamel. *Caries Res* 26:333-339.

Fried D, Glena RE, Featherstone JD, and Seka W. 1997. Permanent and transient changes in the reflectance of CO2 laser-irradiated dental hard tissues at lambda = 9.3, 9.6, 10.3, and 10.6 microns and at fluences of 1-20 J/cm2. *Lasers Surg Med* 20:22-31.

García-Godoy F, and Hicks MJ. 2008. Maintaining the integrity of the enamel surface: the role of dental biofilm, saliva and preventive agents in enamel demineralization and remineralization. *J Am Dent Assoc* 139 Suppl:25S-34S.

Greene VA. 2005. Underserved elderly issues in the United States: burdens of oral and medical health care. *Dent Clin North Am* 49:363-376. 10.1016/j.cden.2004.11.001

Guegan C, Garderes J, Le Pennec G, Gaillard F, Fay F, Linossier I, Herry JM, Fontaine MN, and Rehel KV. 2014. Alteration of bacterial adhesion induced by the substrate stiffness. *Colloids Surf B Biointerfaces* 114:193-200. 10.1016/j.colsurfb.2013.10.010

Hausen H. 1997. Caries prediction--state of the art. *Community Dent Oral Epidemiol* 25:87-96.

Hsu CY, Jordan TH, Dederich DN, and Wefel JS. 2000. Effects of low-energy CO2 laser irradiation and the organic matrix on inhibition of enamel demineralization. *J Dent Res* 79:1725-1730.

Hsu CY, Jordan TH, Dederich DN, and Wefel JS. 2001. Laser-matrix-fluoride effects on enamel demineralization. *J Dent Res* 80:1797-1801.

Kantorowitz Z, Featherstone JD, and Fried D. 1998. Caries prevention by CO2 laser treatment: dependency on the number of pulses used. *J Am Dent Assoc* 129:585-591.

Klein MI, DeBaz L, Agidi S, Lee H, Xie G, Lin AH, Hamaker BR, Lemos JA, and Koo H. 2010. Dynamics of Streptococcus mutans transcriptome in response to starch and sucrose during biofilm development. *PLoS One* 5:e13478. 10.1371/journal.pone.0013478

Klein MI, Duarte S, Xiao J, Mitra S, Foster TH, and Koo H. 2009. Structural and molecular basis of the role of starch and sucrose in Streptococcus mutans biofilm development. *Appl Environ Microbiol* 75:837-841. 10.1128/AEM.01299-08

Koo H, Seils J, Abranches J, Burne RA, Bowen WH, and Quivey RG. 2006. Influence of apigenin on gtf gene expression in Streptococcus mutans UA159. *Antimicrob Agents Chemother* 50:542-546. 10.1128/AAC.50.2.542-546.2006

Loesche WJ. 1986. Role of Streptococcus mutans in human dental decay. *Microbiol Rev* 50:353-380.

462 Lynch DJ, Fountain TL, Mazurkiewicz JE, and Banas JA. 2007. Glucan-binding proteins are
463 essential for shaping Streptococcus mutans biofilm architecture. *FEMS Microbiol Lett*
464 268:158-165. 10.1111/j.1574-6968.2006.00576.x
465 Marcenes W, Kassebaum NJ, Bernabe E, Flaxman A, Naghavi M, Lopez A, and Murray CJ.
466 2013. Global burden of oral conditions in 1990-2010: a systematic analysis. *J Dent Res*
467 92:592-597. 10.1177/0022034513490168
468 Marsh PD. 2003. Are dental diseases examples of ecological catastrophes? *Microbiology*
469 149:279-294. 10.1099/mic.0.26082-0
470 Murata R, and Pardi V. 2007. Is dental caries reaching epidemic proportions in Brazil? Nature
471 Reviews Immunology.
472 Murata RM, Branco-de-Almeida LS, Franco EM, Yatsuda R, dos Santos MH, de Alencar SM,
473 Koo H, and Rosalen PL. 2010. Inhibition of Streptococcus mutans biofilm accumulation
474 and development of dental caries in vivo by 7-epiclusianone and fluoride. *Biofouling*
475 26:865-872. 10.1080/08927014.2010.527435
476 Nelson DG, Shariati M, Glena R, Shields CP, and Featherstone JD. 1986. Effect of pulsed low
477 energy infrared laser irradiation on artificial caries-like lesion formation. *Caries Res*
478 20:289-299.
479 Nelson DG, Wefel JS, Jongebloed WL, and Featherstone JD. 1987. Morphology, histology and
480 crystallography of human dental enamel treated with pulsed low-energy infrared laser
481 radiation. *Caries Res* 21:411-426.
482 Newbrun E. 1977. Control of dental caries. Southern Medical Journal. p 1161-1164.
483 Nobbs AH, Lamont RJ, and Jenkinson HF. 2009. Streptococcus adherence and colonization.
484 *Microbiol Mol Biol Rev* 73:407-450, Table of Contents. 10.1128/MMBR.00014-09
485 Nobre-dos-Santos M, Featherstone J, and Fried D. 2001. Effect of a new carbon dioxide laser
486 and fluoride on sound and demineralized enamel. Proceedings of SPIE- International
487 Society for Optical Engineering. p 169-174.
488 Paris S, Meyer-Lueckel H, Cölfen H, and Kielbassa AM. 2007. Penetration coefficients of
489 commercially available and experimental composites intended to infiltrate enamel carious
490 lesions. *Dent Mater* 23:742-748. 10.1016/j.dental.2006.06.029
491 Perera-Costa D, Bruque JM, Gonzalez-Martin ML, Gomez-Garcia AC, and Vadillo-Rodriguez
492 V. 2014. Studying the influence of surface topography on bacterial adhesion using
493 spatially organized microtopographic surface patterns. *Langmuir* 30:4633-4641.
494 10.1021/la5001057
495 Quirynen M, Bollen CM, Papaioannou W, Van Eldere J, and van Steenberghe D. 1996. The
496 influence of titanium abutment surface roughness on plaque accumulation and gingivitis:
497 short-term observations. *Int J Oral Maxillofac Implants* 11:169-178.
498 Rodrigues LK, Nobre Dos Santos M, and Featherstone JD. 2006. In situ mineral loss inhibition
499 by CO2 laser and fluoride. *J Dent Res* 85:617-621.
500 Rolla G. 1989. Why is sucrose so cariogenic? The role of glucosyltransferase and
501 polysaccharides. *Scand J Dent Res* 97:115-119.
502 Rolland SL, McCabe JF, Robinson C, and Walls AW. 2006. In vitro biofilm formation on the
503 surface of resin-based dentine adhesives. *Eur J Oral Sci* 114:243-249. 10.1111/j.1600-
504 0722.2006.00359.x
505 Sol A, Feuerstein O, Featherstone JD, and Steinberg D. 2011. Effect of sublethal CO2 laser
506 irradiation on gene expression of streptococcus mutans immobilized in a biofilm. *Caries*
507 *Res* 45:361-369. 10.1159/000329390

Song F, and Ren D. 2014. Stiffness of cross-linked poly(dimethylsiloxane) affects bacterial adhesion and antibiotic susceptibility of attached cells. *Langmuir* 30:10354-10362. 10.1021/la502029f

Steinberg D, Moreinos D, Featherstone J, Shemesh M, and Feuerstein O. 2008. Genetic and physiological effects of noncoherent visible light combined with hydrogen peroxide on Streptococcus mutans in biofilm. *Antimicrob Agents Chemother* 52:2626-2631. 10.1128/AAC.01666-07

Steiner-Oliveira C, Rodrigues LK, Soares LE, Martin AA, Zezell DM, and Nobre-dos-Santos M. 2006. Chemical, morphological and thermal effects of 10.6-microm CO2 laser on the inhibition of enamel demineralization. *Dent Mater J* 25:455-462.

Tagliaferro EP, Rodrigues LK, Nobre Dos Santos M, Soares LE, and Martin AA. 2007. Combined effects of carbon dioxide laser and fluoride on demineralized primary enamel: an in vitro study. *Caries Res* 41:74-76. 10.1159/000096109

Taubman MA, and Nash DA. 2006. The scientific and public-health imperative for a vaccine against dental caries. *Nat Rev Immunol* 6:555-563. 10.1038/nri1857

Teughels W, Van Assche N, Sliepen I, and Quirynen M. 2006. Effect of material characteristics and/or surface topography on biofilm development. *Clin Oral Implants Res* 17 Suppl 2:68-81. 10.1111/j.1600-0501.2006.01353.x

Venault A, Yang HS, Chiang YC, Lee BS, Ruaan RC, and Chang Y. 2014. Bacterial resistance control on mineral surfaces of hydroxyapatite and human teeth via surface charge-driven antifouling coatings. *ACS Appl Mater Interfaces* 6:3201-3210. 10.1021/am404780w

Wang Q, Jia P, Cuenco KT, Feingold E, Marazita ML, Wang L, and Zhao Z. 2013. Multi-dimensional prioritization of dental caries candidate genes and its enriched dense network modules. *PLoS One* 8:e76666. 10.1371/journal.pone.0076666

Weber K, Delben J, Bromage TG, and Duarte S. 2014. Comparison of SEM and VPSEM imaging techniques with respect to Streptococcus mutans biofilm topography. *FEMS Microbiol Lett* 350:175-179. 10.1111/1574-6968.12334

WHO. 2003. The world Oral Health Report. Continuous improvement of oral health in the 21 st century - the approach of the WHO global oral health programme.

Zero DT, van Houte J, and Russo J. 1986. Enamel demineralization by acid produced from endogenous substrate in oral streptococci. *Arch Oral Biol* 31:229-234.

554
555

Table 1(on next page)

Primers used for RT-qPCR.

GenBank Locus Tag	Gene Name	Primer sequence (forward and reverse)
	16S rRNA	ACCAGAAAGGGACGGCTAAC
		TAGCCTTTTACTCCAGACTTTCCTG
SMU.1004	*gtfB*	AAACAACCGAAGCTGATAC
		CAATTTCTTTTACATTGGGAAG
SMU.22	*gbpB*	ATACGATTCAAGGACAAGTAAG
		TGACCCAAAGTAGCAGAC

1

Table 2 (on next page)

The content of CFU/mL, Dry Weight (mg/ mL), CFU/ Dry Weight in *S. mutans* biofilm. Data represent the mean values and standard deviations.

1

	Biofilm					
	Day 3			Day 5		
Groups	CFU/mL	Dry Weight (mg/ mL)	CFU/ Dry Weight	CFU/mL	Dry Weight (mg/ mL)	CFU/ Dry Weight
Control	8.60 ± 0.33[a]	6.55 ± 0.37[a]	7.80 ± 0.31[a]	7.72 ± 0.29[a]	10.41 ± 0.92[a]	6.70 ± 0.29[a]
Laser	7.78 ± 0.16[b]	6.70 ± 0.64[a]	6.99 ± 0.08[b]	7.67 ± 0.29[a]	11.38 ± 5.72[a]	4.31 ± 1.16[a]

PeerJ Preprints | https://doi.org/10.7287/peerj.preprints.2084v1 | CC-BY 4.0 Open Access | rec: 30 May 2016, publ: 30 May 2016

Table 3(on next page)

The content of EPS-soluble, EPS-insoluble in *S. mutans* biofilm (expressed in µg/mg of biofilm). Data represent the mean values and standard deviations.

Values marked by the different letters are significantly different from each other ($p > 0.05$). T-test was employed for soluble polysaccharide and Mann Whitney test for insoluble polysaccharide.

1

	Polysaccharides (µg PSA/ mg dry weight)			
	Soluble		Insoluble	
Groups	Day 3	Day 5	Day 3	Day 5
Control	4.92 ± 1.51[a]	4.89 ± 2.13[a]	7.20 ± 1.33[a]	8.84 ± 2.80[a]
Laser	4.32 ± 1.29[a]	4.31 ± 1.27[a]	8.20 ± 2.92[a]	8.93 ± 1.31[a]

Table 4(on next page)

The content of Contact Angle. mutans biofilm. Data represent the mean values of angle (°) and standard deviations.

Values marked by the different letters are significantly different from each other. T-test ($p < 0.05$).

1

Groups	Contact Angle (°)
Control	76.0 ± 3.33[a]
Laser	87.6 ± 9.41[b]

Figure 1(on next page)

Flowchart of the experimental design of the study.

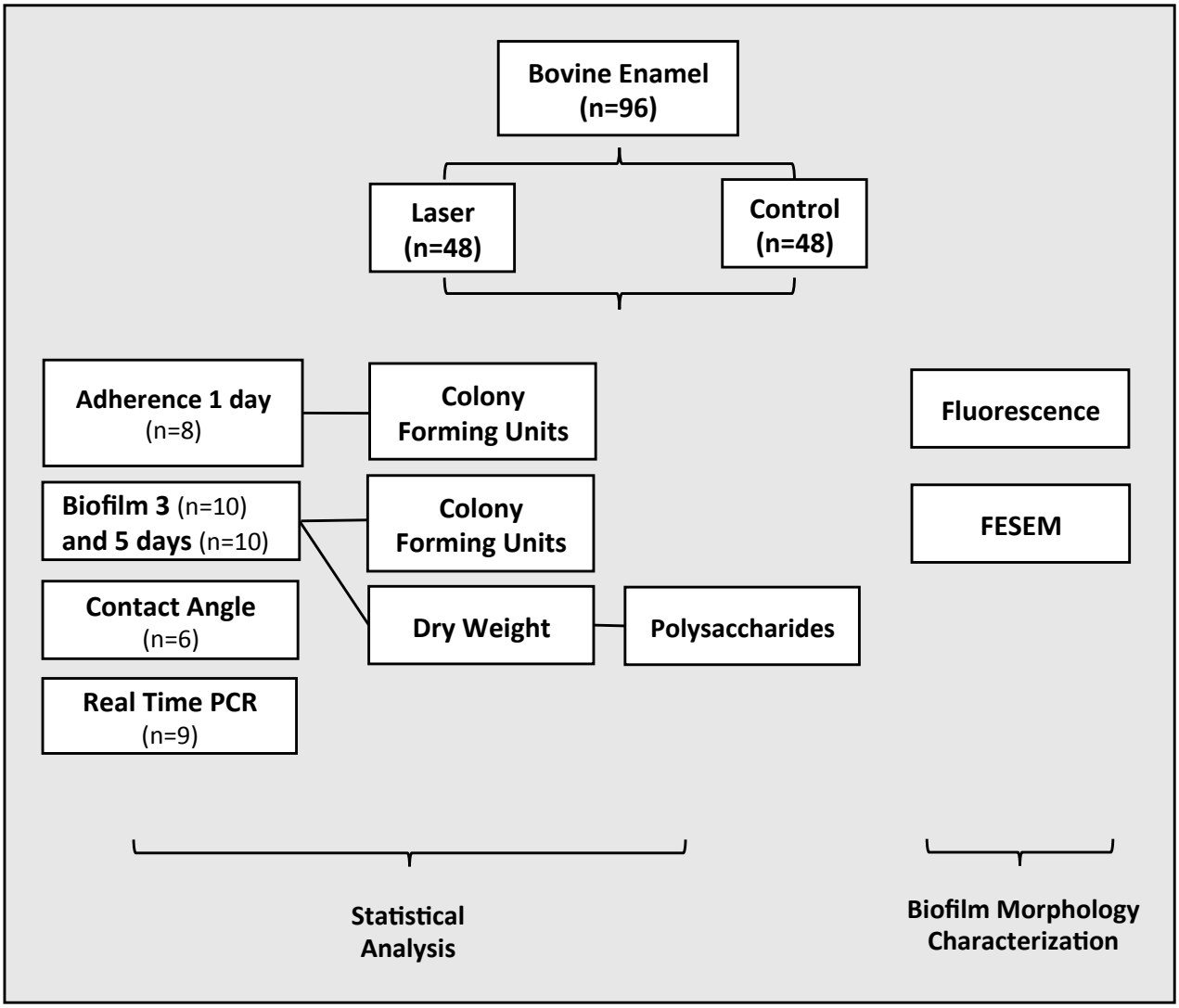
Bovine Enamel (n=96)
Laser (n=48)
Control (n=48)
Adherence 1 day (n=8)
Colony Forming Units
Biofilm 3 (n=10) and 5 days (n=10)
Colony Forming Units
Contact Angle (n=6)
Dry Weight
Polysaccharides
Real Time PCR (n=9)
Fluorescence
FESEM
Statistical Analysis
Biofilm Morphology Characterization

Figure 2(on next page)

Overlaping area of laser irradiation between points.

PeerJ Preprints | https://doi.org/10.7287/peerj.preprints.2084v1 | CC-BY 4.0 Open Access | rec: 30 May 2016, publ: 30 May 2016

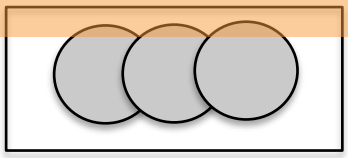

PeerJ Preprints | https://doi.org/10.7287/peerj.preprints.2084v1 | CC-BY 4.0 Open Access | rec: 30 May 2016, publ: 30 May 2016

Figure 3(on next page)

Streptococcus mutans adherence test performed in day 1 of biofilm (expressed in log CFU/mL). Values marked by the distinct letters are significantly different from each other. T-test ($p < 0.05$).

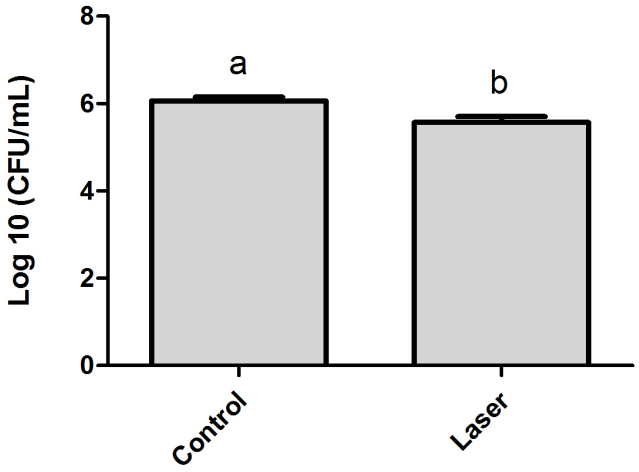

Figure 4(on next page)

Real time quantitative information about gene expression in S. mutans biofilm after treatments with/without laser irradiation on enamel surface.

A. gtfB B. gbpB. Values marked by the same letters are not significantly different from each other ($p > 0.05$). T-test ($p > 0.05$).

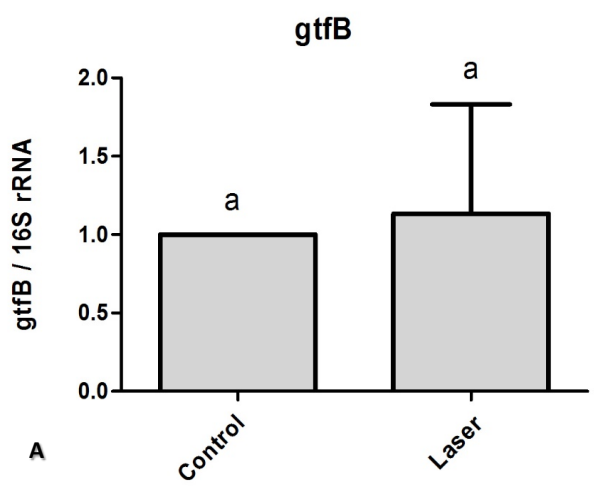
gtfB
gtfB / 16S rRNA
2.0
1.5
1.0
0.5
0.0
a
a
Control
Laser
A

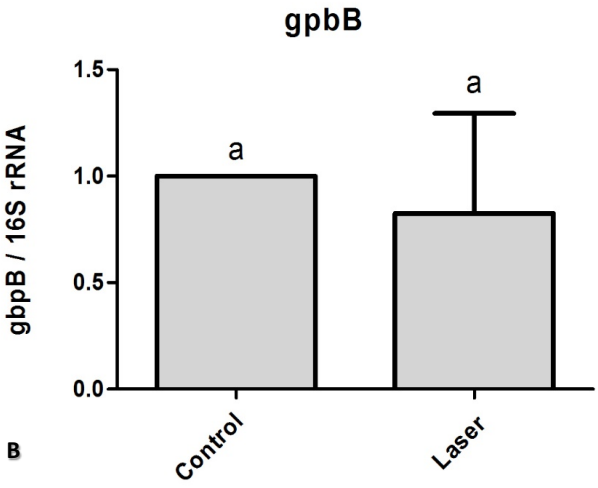
gpbB
gbpB / 16S rRNA
1.5
1.0
0.5
0.0
a
a
Control
Laser
B

Figure 5(on next page)

Fluorescence Microscopy showing representative images of bacteria in biofilms after 1, 3 and 5 days of biofilm. Multidimensional imaging of live (green) and dead (red) bacteria.

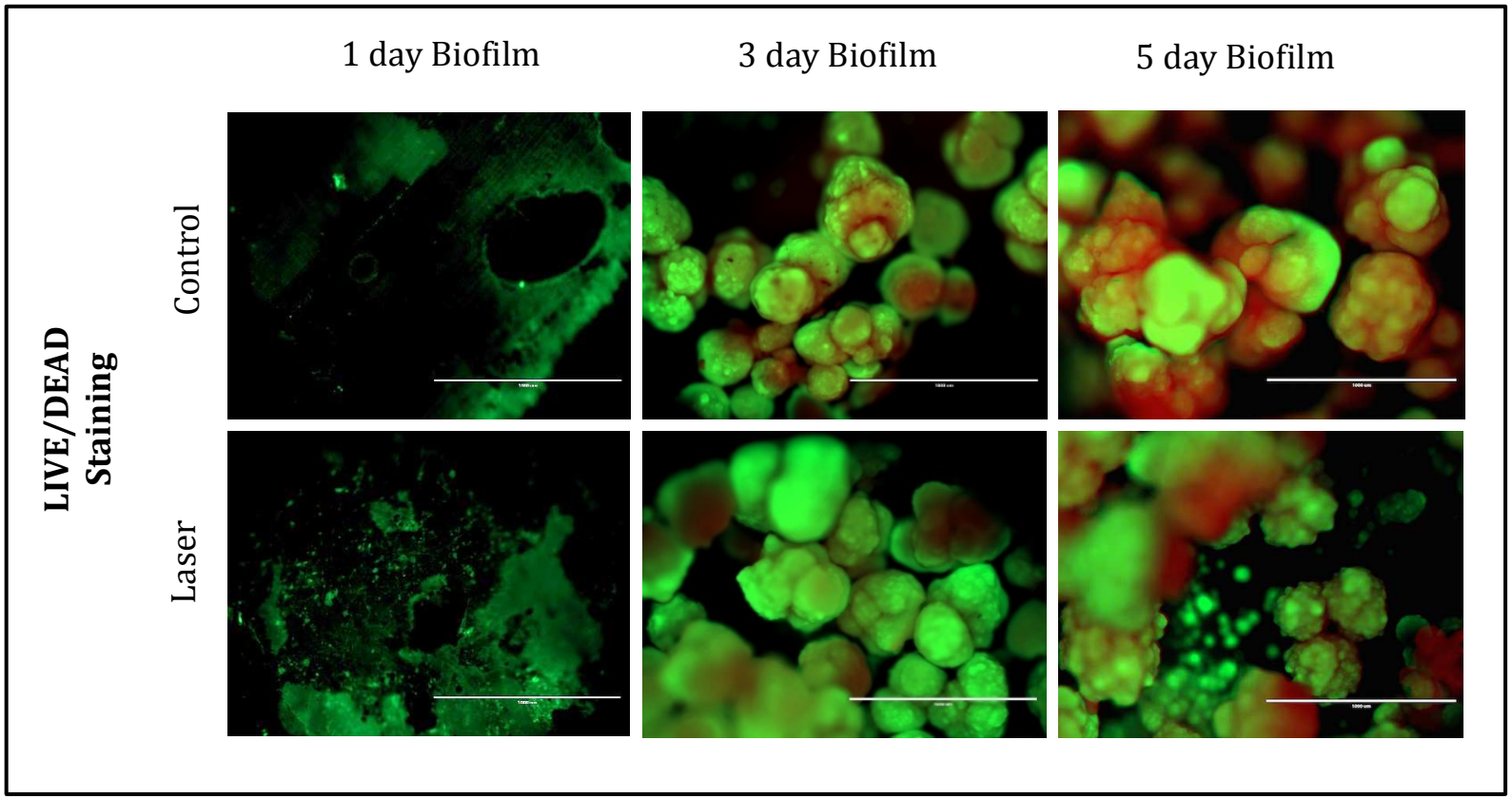

PeerJ Preprints | https://doi.org/10.7287/peerj.preprints.2084v1 | CC-BY 4.0 Open Access | rec: 30 May 2016, publ: 30 May 2016

Figure 6(on next page)

Morphology and structure of after 1, 3 and 5 days S. mutans biofilms imaged by FESEM (2500X).

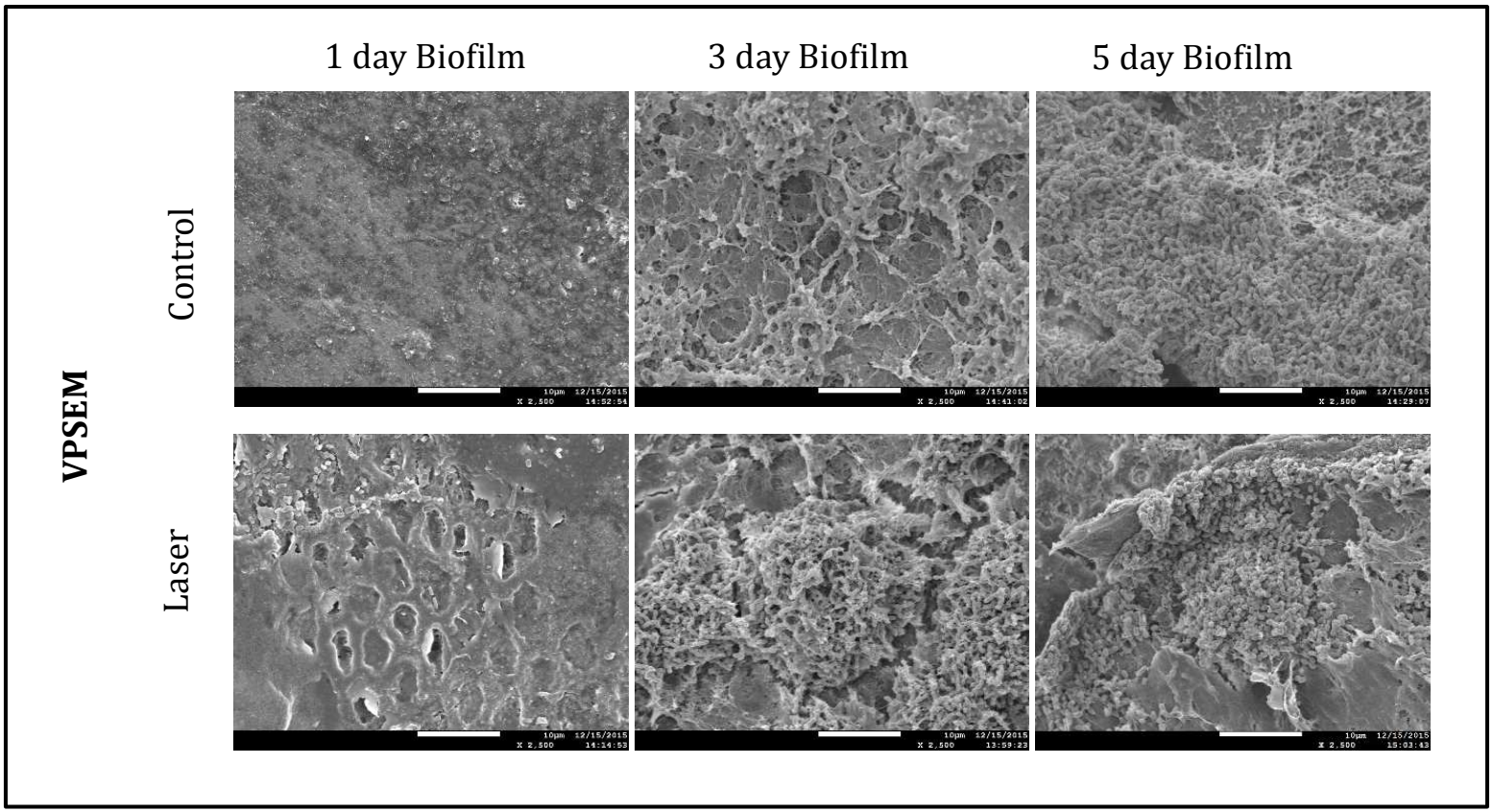

PeerJ Preprints | https://doi.org/10.7287/peerj.preprints.2084v1 | CC-BY 4.0 Open Access | rec: 30 May 2016, publ: 30 May 2016